ORIGINAL RESEARCH

Platelet Membrane Biomimetic Manganese Carbonate Nanoparticles Promote Breast Cancer Stem Cell Clearance for Sensitized Radiotherapy

Yi Jiang [1],*, Xiaoming Liao[1],*, Wei Tang[2], Chunyu Huang[3], You Pan[2], Shipeng Ning[2]

[1]Department of Breast Surgery, Guangxi Medical University Cancer Hospital, Nanning, 530000, People's Republic of China; [2]Department of Breast Surgery, The Second Affiliated Hospital of Guangxi Medical University, Nanning, 530000, People's Republic of China; [3]Key Laboratory of Artificial Micro- and Nano-Structures of Ministry of Education, School of Physics and Technology, Wuhan University, Wuhan, 430072, People's Republic of China

*These authors contributed equally to this work

Correspondence: Shipeng Ning, Email nspdoctor@sr.gxmu.edu.cn

Introduction: The presence of cancer stem cells (CSCs) significantly limits the therapeutic efficacy of radiotherapy (RT). Efficient elimination of potential CSCs is crucial for enhancing the effectiveness of RT.

Methods: In this study, we developed a biomimetic hybrid nano-system (PMC) composed of $MnCO_3$ as the inner core and platelet membrane (PM) as the outer shell. By exploiting the specific recognition properties of membrane surface proteins, PMC enables precise targeting of CSCs. Sonodynamic therapy (SDT) was employed using manganese carbonate nanoparticles ($MnCO_3$ NPs), which generate abundant reactive oxygen species (ROS) upon ultrasound (US) irradiation, thereby impairing CSC self-renewal capacity and eradicating CSCs. Subsequent RT effectively eliminates common tumor cells.

Results: Both in vitro cell experiments and in vivo animal studies demonstrate that SDT mediated by PMC synergistically enhances RT to selectively combat CSCs while inhibiting tumor growth without noticeable side effects.

Discussion: Our findings offer novel insights for enhancing the efficacy and safety profiles of RT.

Keywords: cancer stem cells clearance, radiosensitization, platelet membrane, sonodynamic therapy, manganese carbonate nanoparticles

Introduction

Although researchers have made remarkable progress in cancer biology, oncology and surgery in recent years, cancer remains one of the major diseases that lead to human death.[1,2] Among them, radiotherapy (RT) represents the predominant therapeutic approach, with approximately half of cancer patients opting for this modality either as a standalone treatment or in combination with other modalities to effectively manage cancer.[3] During RT, radiation ionization can generate free radicals, and then cause irreversible DNA damage.[4,5] Despite the widespread utilization of radiotherapy (RT) in cancer treatment, there persist several limitations. Due to the tumor's limited capacity for radiation absorption, high-intensity radiation is often required for effective tumor eradication, potentially leading to collateral damage in adjacent normal tissues.[6,7] Furthermore, the eradication of tumor cells is challenging in radiation therapy, and cancer recurrence and metastasis are the primary causes of death.[8] According to reports, cancer stem cells (CSCs) are closely related to the endless growth of tumors and the failure of RT.[9] CSCs are a small number of cells with infinite proliferation, self-renewal and multidirectional differentiation in tumor tissues.[10] The heterogeneity, special tumor microenvironment (TME), gene instability and flexible self-protection ability of CSCs can largely avoid the damage caused by RT.[11] CSCs can survive under high-dose radiation by regulating redox homeostasis, eliminating highly toxic ROS, repairing DNA damage and changing its division mode.

Therefore, it is of great significance for cancer treatment to effectively eliminate differentiated cancer cells and potential CSCs. As most CSCs are located in the oxygen-deficient area of solid tumors, it is difficult for conventional nano-preparations and chemotherapy drugs to break through the physical barrier, resulting in limited killing effect on CSCs.[12] In recent years, the bionic technology of cell membrane camouflage nanoparticles has been attracting increasing attention.[13–15] Biomimetic nano-systems disguised by cell membrane have the advantages of excellent biocompatibility, prolonged blood circulation time and avoiding the immunity of the internal immune system.[16] This bionic camouflage technology not only accurately replicates the diverse antigens on the cell membrane surface (CD20, CD44, CD90, CD133, etc.), but also significantly simplifies the complex modification process of multifunctional nanoparticles.[17] Among them, platelet membrane-based biomimetic nanomaterials (PMN) based on platelet membrane can effectively target CD44 protein on the surface. PMN can target tumor tissue efficiently by P-selectin (CD62p)-CD44 binding on the platelet membrane.[18,19] For example, in the previous study, composite hybrid system (named PMT) was prepared by loading photosensitiser into mesoporous organosilicon nanoparticles (MON) and further modifying the platelet membrane.[12] Furthermore, Chen et al designed a copper-doped hybrid bionic nanoparticles for enhanced low-temperature photothermal therapy.[20] PMT can cooperate with photodynamic therapy (PDT) to achieve specific killing of CSCs. Therefore, nano-systems based on platelet membrane modification are promising for CSCs killing.

Sonodynamic therapy (SDT) is considered one of the most promising therapeutic strategies due to its high tumor specificity, excellent controllability, significant therapeutic effect, and minimal damage to normal organs or tissues.[21] As sound waves penetrate deeper into tissues, sonodynamic therapy is suitable for large tumors that are difficult to be treated by phototherapy.[22,23] This method can cooperate well with RT to achieve a safer and more efficient effect. The stability of widely reported sonosensitizers such as porphyrin derivatives (hematoporphyrin, phthalocyanine, etc.) under ultrasonic action is often limited, and most sound-sensitive molecules are also photosensitizers, which are harmful to human body in cancer treatment because of their phototoxicity and skin sensitivity.[24] As a representative of inorganic sonosensitizers, TiO_2 exhibits favorable chemical stability and water solubility; however, its metabolic challenges and rapid electron–hole recombination rate impede its further application in SDT.[25,26] It is worth noting that Liu et al developed a new type of nano-sonosensitizers manganese carbonate ($MnCO_3$) to achieve excellent SDT.[27] The excellent biodegradability, simple and feasible preparation method, as well as potent ROS production ability of $MnCO_3$ provide strong motivation for targeting CSCs with $MnCO_3$ coated platelet membrane to achieve synergistic treatment of RT and SDT.

In this study, we developed a biomimetic nanoplatform camouflaged with platelet cell membranes for targeted delivery of $MnCO_3$ NPs to the deep-seated CSC area within tumors, thereby achieving potent SDT and RT (Scheme 1). The $MnCO_3$ NPs were synthesized using the inverse microemulsion method. Subsequently, we modified the surface of $MnCO_3$ NPs with platelet membrane possessing immune evasion capability and active targeting ability to create a hybrid nano-system (named PMC). Upon intravenous administration, PMC exhibited enhanced accumulation in tumor tissue, particularly in CSCs, through specific recognition between surface proteins (P-selectin (CD62p)) on tumor cells (CD44). Under ultrasound activation, PMC generated various reactive oxygen species such as singlet oxygen ($^1O_2$) and hydroxyl radical (OH), leading to selective eradication of CSCs and other tumor cells while synergizing with low-dose RT to suppress tumor growth. In vitro and in vivo experiments demonstrated that combined treatment involving PMC, US irradiation, and 4 Gy RT exerted remarkable synergistic anti-tumor effects without compromising biological safety. Our findings provide novel insights into improving both efficacy and safety profiles of RT.

Results and Discussion

We prepared $MnCO_3$ NPs via simple inverse microemulsion method. Transmission electron microscopy (TEM) can observe fine structures at the nanoscale.[28] As shown in Figure 1A, the TEM analysis revealed the successful synthesis of $MnCO_3$ nanoparticles with a cubic structure, exhibiting an average particle size of approximately 80 nm. The obtained $MnCO_3$ NPs have a uniform particle size, which makes it easier to functionalize. Subsequently, the synthesized material was modified with a platelet membrane. As illustrated in Figure 1A, PMC had an obvious membrane coating on its surface, which increased its particle size by about 8 nm. To further demonstrate the success of platelet membrane modification, western blot (WB) analysis was used to verify whether PMC retained platelet membrane specific proteins. The results (Figure 1B) showed that PMC was detected to obtain P-selectin (CD62p), which is key protein targeting
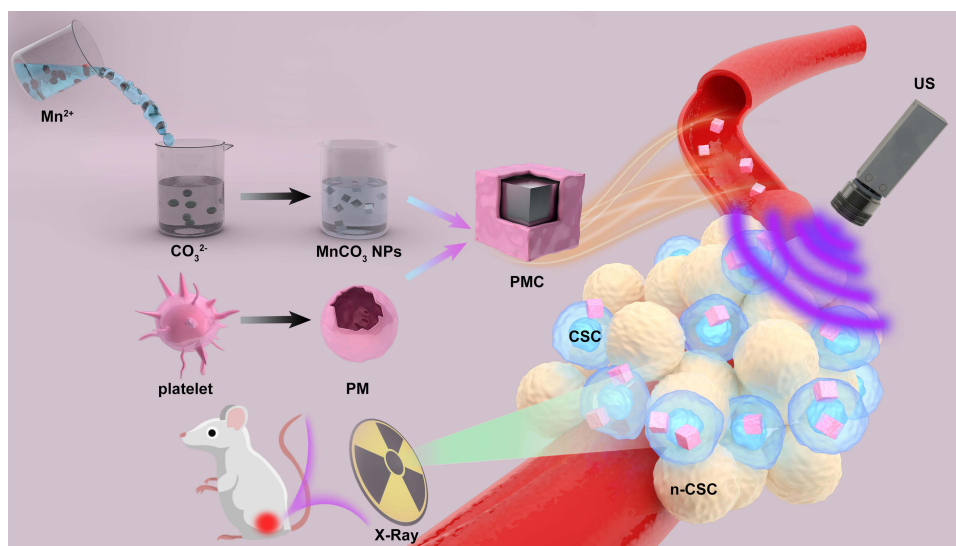
Scheme 1 Schematic diagram of PMC for eradicating CSCs and enhanced RT.

tumor cells, and CD41 protein. The outermost membrane coating of the PMC nanostructure retains the proteins on the normal platelet membrane, ensuring the functional integrity of the membrane. Elemental mapping images (Figure 1C) further proved the homogeneous distribution of C, Mn, and O elements within $MnCO_3$. The X-ray diffraction pattern (XRD) in Figure 1D shows the crystalline structures of $MnCO_3$, all characteristic peaks from 20° to 80° were consistent with standard card of powder $MnCO_3$ (JCPDS No.44–1472). In view of the clear structure of PMC, we continued to verify its function under US irradiation, using methylene blue (MB) and 1.3-Diphenylisobenzofuran (DPBF) as indicators to explore the ability of PMC to produce different kinds of ROS (Figure 1E and F). When MB was incubated with PMC alone, it was found that MB did not degrade. In addition, US alone could not produce OH. Notably, when $MnCO_3$ NPs were co-incubated with MB, the characteristic absorption peak of the mixed solution is significantly reduced after US irradiation, indicating that $MnCO_3$ NPs could cooperate with US to produce OH. In addition, similar results were observed in the PMC + MB + US group, namely, the coating of platelet membrane would not affect the function of $MnCO_3$. To continuously evaluate the ability of PMC as a sonosensitizer, $^1O_2$ production was demonstrated using a DPBF probe, which demonstrated that PMC could oxidize DPBF under ultrasonic irradiation to reduce the characteristic absorbance at 410 nm (Figure 1F), which proved that PMC could generate $^1O_2$ under US irradiation. As shown in Figures S1 and S2, under the conditions of pH = 6.5, $MnCO_3$ NPs were nearly degraded within 24 h. The uptake of PMC by 4T1 CSC was analyzed by confocal laser scanning microscope (CLSM). The expression of CD133 in different cells was shown in Figure S3. Erythrocyte membrane coated $MnCO_3$ NPs (named RMC) was used as control. Erythrocyte membrane has long blood circulation,[29,30] but it lacks specific proteins to actively target tumor cells. After RMC and PMC were incubated with cells (Figure 1G), RMC was rarely endocytosed by CSC, while PMC was highly enriched to CSC (Figure S4). These results indicate that the cell membrane on the surface of PMC imparts active targeting capabilities to nanoparticles. Similarly, flow cytometry analysis yielded consistent results (Figure 1H).

In view of the good material characterization effect and the fact that PMC is effectively swallowed by CSC. We continue to explore the effect of PMC on enhancing radiotherapy at the cellular level in vitro. For enhanced-RT, the following groups were used for exploratory experiments: (1): PBS + US; (2): RT; (3): PMC; (4): RMC + US + RT; (5): PMC + US and (6): PMC + US + RT. The dose of RT is 4 Gy. Then, cell cloning experiment was utilized to analyze the synergistic therapeutic ability of SDT and RT mediated by PMC (Figure 2A). Compared with PBS + US group, RMC + RT + US group and PMC + US group showed fewer cell clones, and the cell division of PMC + US + RT group was most effectively inhibited. The quantitative results of survival scores also show consistent results (Figure 2B). CSCs with self-protection ability can largely avoid the damage to RT and contribute to the failure of follow-up treatment, so it is of great significance to effectively eliminate differentiated cancer cells and potential CSCs for the cure of cancer.[31] The effects of
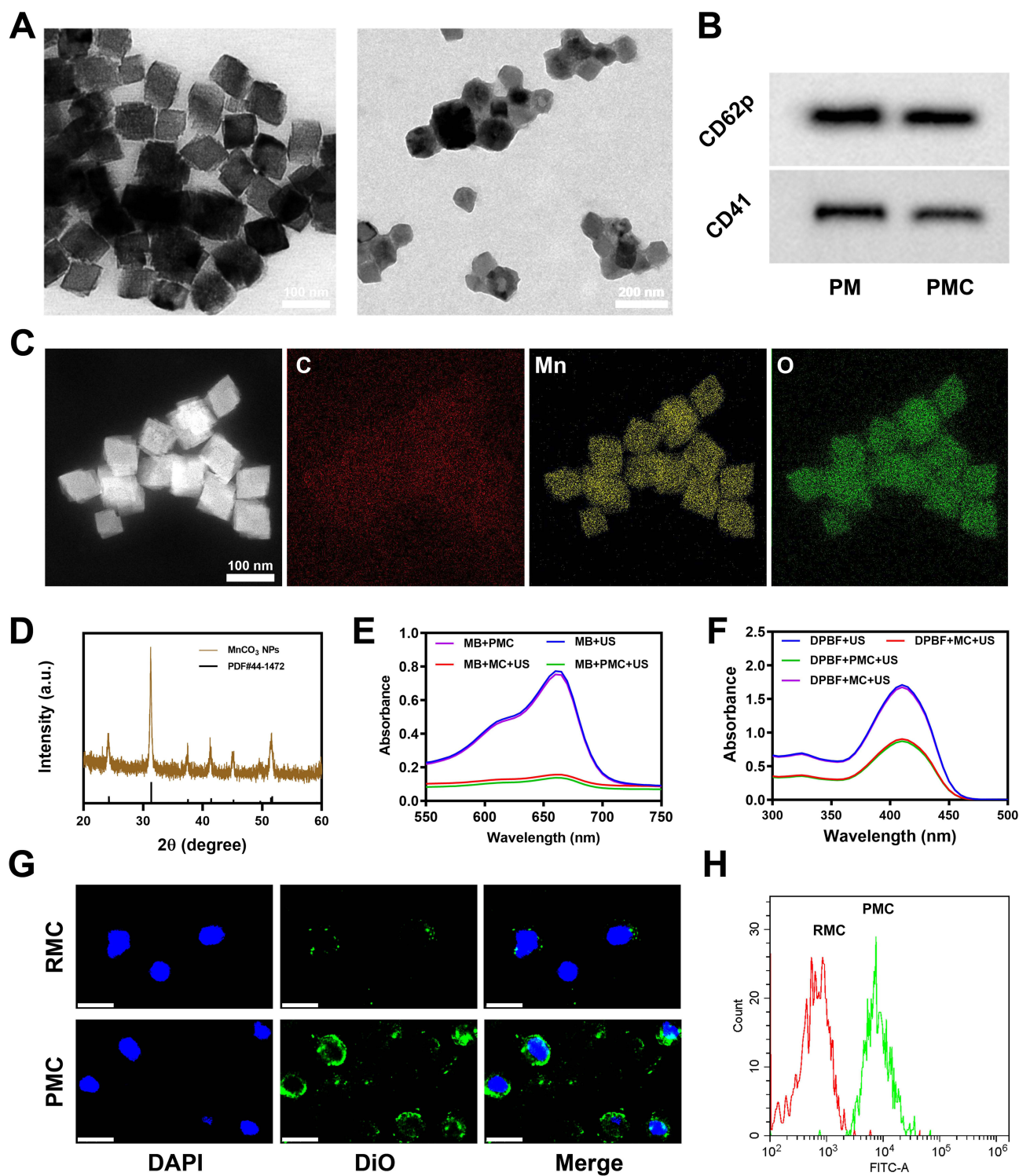
Figure 1 Characterization of PMC. (**A**) TEM image of MnCO₃ and PMC NPs. (**B**) PM markers, including CD41 and CD62p, were detected using Western blotting. (**C**) HAADF-STEM image and the corresponding elemental mapping images of PMC. (**D**) The XRD patterns of PMC. (**E**) The degradation of MB caused by the generation of OH with different groups. (**F**) DPBF was used to detect $^1O_2$ generation in different groups. (**G**) CLSM images of 4T1 CSC incubated with DiO labelled RMC or PMC for 1 h. Blue: DAPI; Green: DiO. Scale bars: 20 μm. (**H**) DiO fluorescence intensity of 4T1 CSC after incubated with indicated nanoparticles.

PMC on CSC proliferation using a stem cell spheroidization assay (Figure 2C). As shown in Figure 2C, RT alone would not inhibit stem cells from forming spheres, but the spheroid formation rate of RMC + US + RT group was still about 30% after treatment. In striking contrast, no obvious stem cell spheroidization was found after the treatment PMC + US + RT group. This result showed that compared with other control groups, PMC + US + RT group had the greatest inhibitory
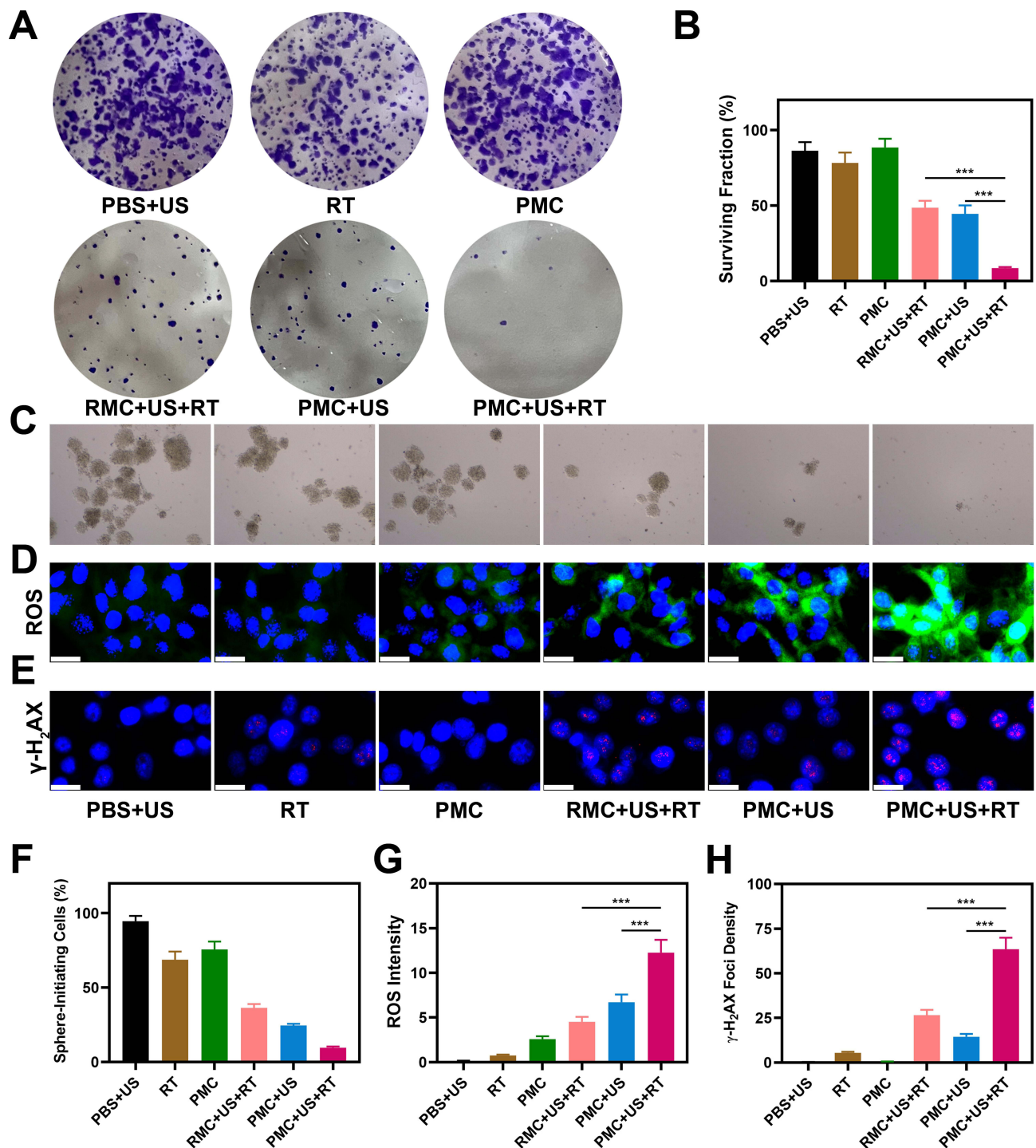
Figure 2 In vitro anti-tumor study. (**A**) Colony of 4T1 cells treated with different formulations. (**B**) Colony formation assays were conducted using 4T1 cells treated with 4 Gy of radiation. (**C**) Sphere-formation assays using 4T1 CSC cultured with various treatments. (**D**) Tumor cells DCFH-DA fluorescence images were observed after the indicated treatments. (**E**) Nuclear condensation and DNA fragmentation were visualized using DAPI and γ-H₂AX staining in cells treated as indicated, with representative pictures presented. (**F**) The numbers of tumor spheres were counted after various treatments. (**G**) CLSM images of intracellular ROS in 4T1 cells after different treatments. (**H**) Quantification of γ-H₂AX foci density in different treatment groups. ***P < 0.001; Student's *t*-test.

effect on stem cell spheroidization (Figure 2F). A fluorescent probe (DCFH-DA) was utilized to detect ROS production in various groups. As shown in the Figure 2D and 2G, PMC + US + RT group induced the brightest green fluorescence. Immunofluorescence technique of 4T1 cells with different treatments was carried out by using γ-H₂AX, a signal molecule of DNA damage, to evaluate the degree of DNA damage induced by different groups (Figure 2E). With the

above results. The cells treated with PMC + US + RT and then incubated showed the most obvious DNA damage after being irradiated by X-rays (Figure 2H). Overall, PMC combined with RT could efficiently induce ROS and DNA damage to combat CSCs and 4T1 tumor cells after US irradiation, providing experimental basis for subsequent in vivo treatment.

PMC has been observed to have effective targeting effect and positive therapeutic effect in vitro, and we further studied its biological effect in vivo. The protein on the surface of RMC lacks specificity, which makes it hard to recognize tumor cells, especially CSCs, and it is difficult for RMC to actively gather in tumor sites. Notably, there is CD62p protein on the surface of PMC (Figure 3A); after intravenous injection, a large number of PMC gather near cells with increased expression level of CD133. The biodistribution profiles of RMC and PMC in tumor tissues and major organs (heart, liver, spleen, lung and kidney) were subsequently detected. Although owning long circulation, RMC group mainly accumulated in liver and kidney tissues with immune clearance function, but the content in tumor tissues is low. Simultaneously, PMC group showed high-performance accumulation in tumor tissue compared with the former (Figure 3B). As shown in Figure S5, in tumor tissue, PMC penetrates farther from blood vessels. The main organs and blood of PMC + US + RT-treated mice were collected for H&E staining and biochemical analysis. The results showed that compared with the healthy mice with PBS + US treatment, no obvious tissue damage was found in PMC + US + RT group (Figure 3C). Blood biochemistry data including kidney function markers and liver function markers indicated that the liver and kidney function were normal (Figure 3D–F). This result showed that PMC had good
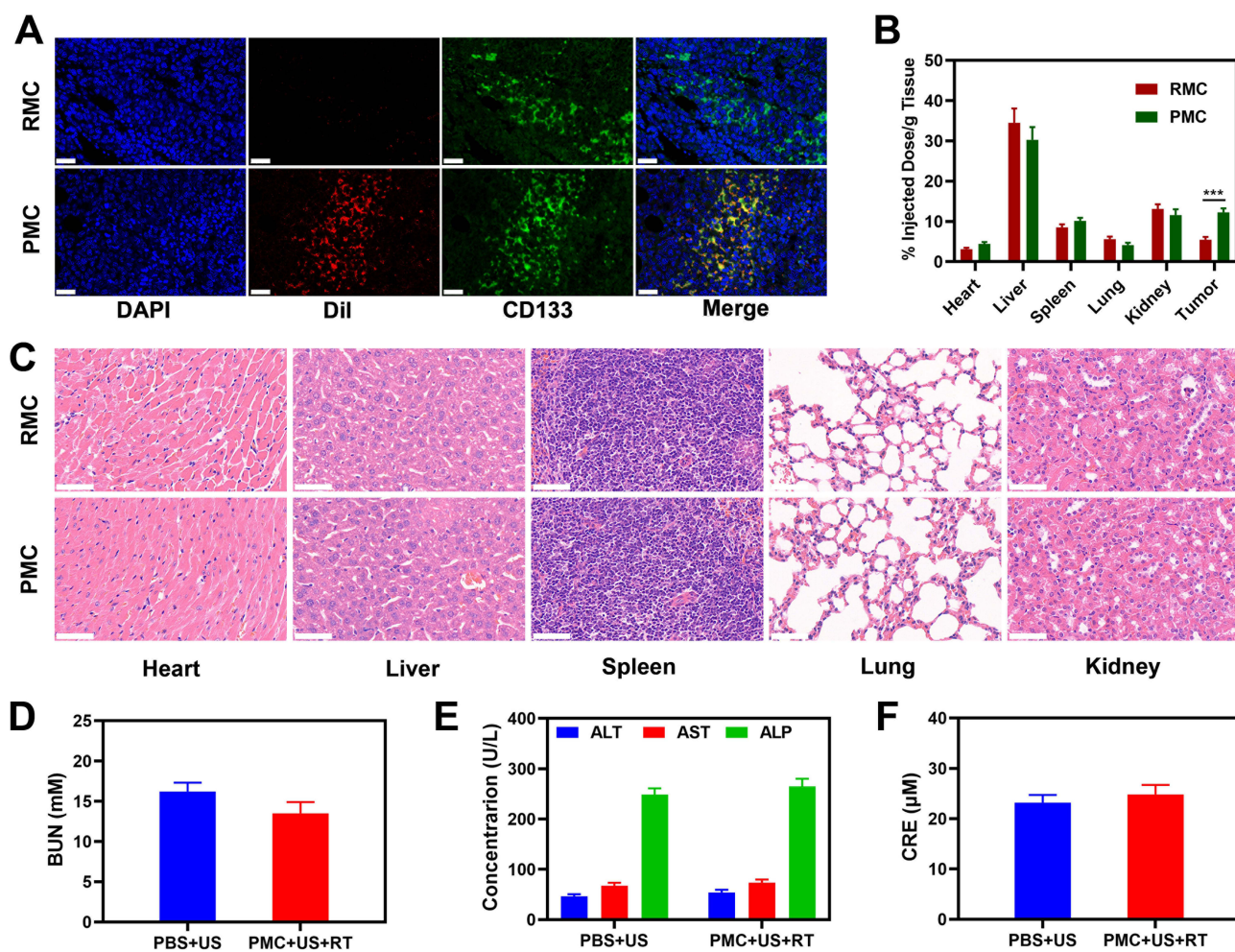

Figure 3 Result of in vivo safety experiments. (**A**) Colocalization of DiI (red), CD133 antibody-labelled cancer cells (green) and nucleus (blue) in tumor sections of 4T1 tumor-bearing mice 12 h after intravenous administration of indicated nanoparticles. Scale bars: 50 μm. (**B**) Biodistribution profile of Mn element in the main organs and tumor tissues at 12-h post-injection with different nanoparticles. (**C**) Histopathological analysis results of (H&E) stained images of the major organs (heart, lung, liver, kidneys, and spleen) of mice that were exposed to different treatments 16 days post-injection under laser irradiation. Scale bars: 100 μm. Blood biochemistry data including kidney function markers and liver function markers: (**D**) BUN, (**E**) ALT, AST and ALP, and (**F**) CRE after various treatments. ***P < 0.001; Student's *t*-test.

compatibility and no harm to the health of mice. Nano-preparations with good biocompatibility are very important for their future biomedical applications. Although many preparations have certain functionality, the accompanying physiological toxicity limits their subsequent applications.[32,33]

Next, we explore whether the tumor-killing effect in vivo is consistent with that in vitro. Female Balb/c mice aged 4–5 week were purchased from Vital River Company (Beijing, China). One hundred μL of 4T1 cell suspension (1×10^6 cells) was subcutaneously injected into each mouse to establish the tumor models. The animal experiments were carried out according to the guidelines approved by the Ministry of Health in People's Republic of PR China (Name of the guidelines followed for the welfare of the laboratory animals: "Laboratory Animal-Guideline for ethical review of animal welfare (GB/T 35892–2018)") and were approved by the Administrative Committee on Animal Research of Wuhan University. When the tumor of 4T1 subcutaneous tumor-bearing mice reached 200mm^3, the mice were randomly divided into 6 groups for treatment: (1): PBS + US; (2): RT; (3): PMC; (4): RMC + US + RT; (5): PMC + US and (6): PMC + US + RT. The dose of RT is 4 Gy. US irradiation (1.0 MHz, 1.5W/cm^2, 50% duty cycle, 5 min) was performed. As shown in Figure 4A, the tumor volume of mice in the group of US, RT or PMC alone increased indefinitely. On the one hand, it exhibited that our PMC is safe and non-toxic. In addition, it is widely acknowledged that US is a non-therapeutic means.[34,35] Although RT is a clinical method, radiotherapy alone would not cure the tumor, and under the influence of various factors, the tumor will proliferate more rapidly, so on the other hand, it showed that a single model hardly achieved the therapeutic purpose. In contrast, the tumor volume of RMC + US + RT group and PMC + US group was moderately limited, which indicated that PMC + US played a role in SDT to some extent. However, in RMC + US + RT,
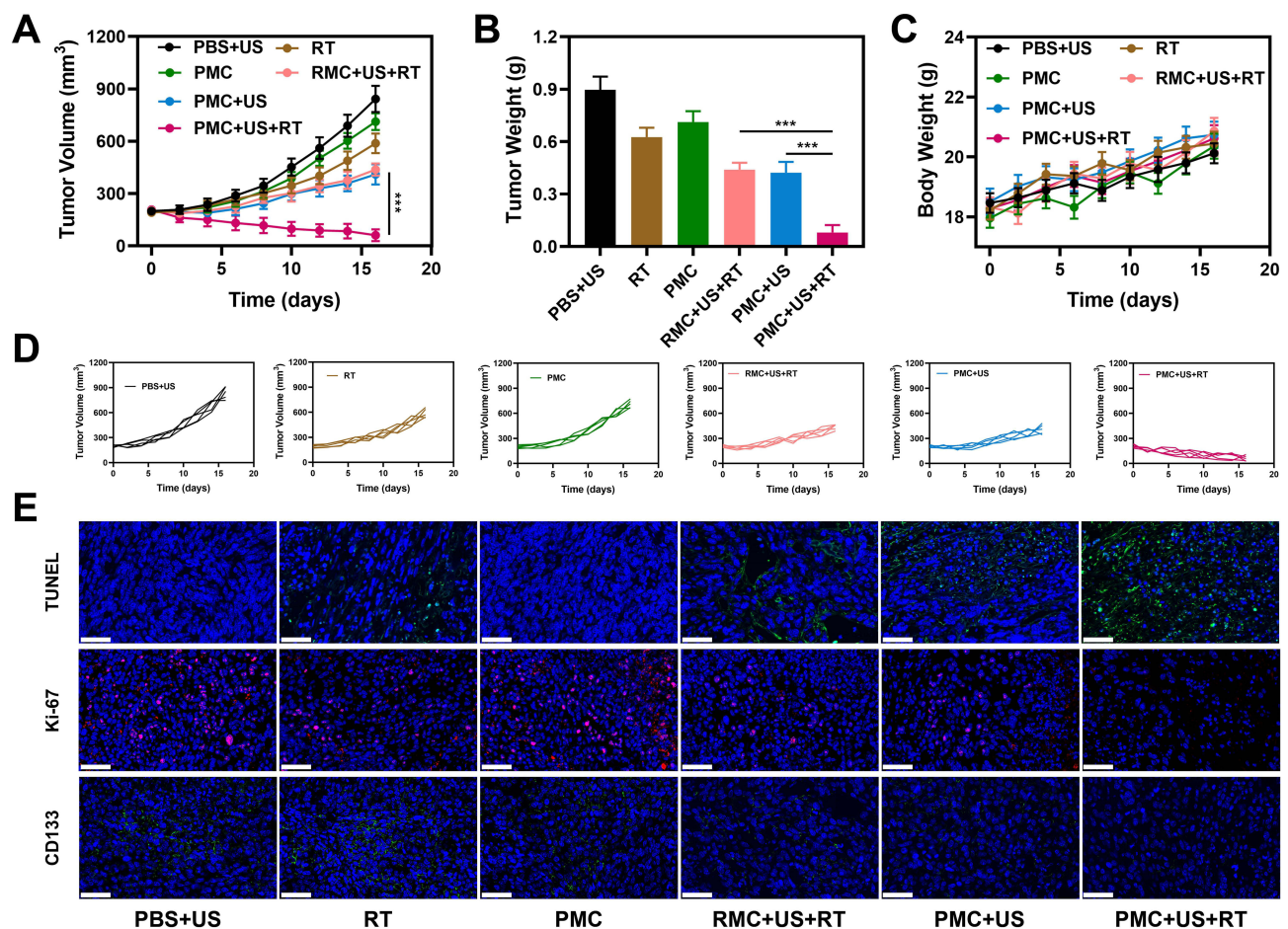

Figure 4 In vivo anti-tumor study. (**A**) Changes in tumor volume over the experimental period. (**B**) Average tumor weights following treatment. (**C**) The body weight of 4T1 tumor-bearing mice was measured every 2 days after therapy. (**D**) Individual rechallenge of 4T1 tumor volume curves. (**E**) TUNEL, Ki-67 and CD133 stained tumor sections from the indicated treatment groups. Scale bars: 50 μm. ***P < 0.001; Student's *t*-test.

as the erythrocyte membrane on the surface of $MnCO_3$ proteins with atopic recognition function to actively target CSCs, so after tumor cells are damaged, CSCs continued play a functional role and tumor volume keep up proliferating indefinitely. Unsurprisingly, PMC can target CSCs and achieve double killing. As shown in PMC + US + RT group, the tumor volume is completely suppressed (Figure 4A). After treatment, the mice were sacrificed and tumors were weighed. The result is consistent with above data, and the tumor weight was significantly reduced in the PMC + US + RT group (Figure 4B). During the treatment, the physical health of mice in each group was observed every 2 days and weighed. As shown in Figure 4C, the weight of mice in all groups increased steadily without death. There was no significant difference in the tumor growth curve of mice in each group (Figure 4D). Subsequently, the dissected tumors in each group were stained, and their histological changes were evaluated. As shown in Figure 4E, in comparison to other groups, the tumor proliferation in PMC + US + RT group was severely restricted, and a number of cells were apoptotic. In a word, PMC can cooperate with RT and US to achieve good tumor treatment effect, accompanied by biological safety.

Conclusions

In conclusion, we have developed a biomimetic hybrid nano-system (PMC) capable of effectively damaging cancer stem cells (CSCs) and enhancing radiotherapy (RT). PMC consists of an inner core composed of $MnCO_3$ and an outer shell made from platelet membrane. The incorporation of platelet membrane provides PMC with excellent biocompatibility and active targeting ability, enabling precise eradication of CSCs. In vitro experiments demonstrated that the combination treatment involving PMC, ultrasound (US), and RT completely inhibited stem cell formation. Furthermore, in vivo experiments successfully validated the synergistic effect between low-dose RT and PMC in suppressing tumor growth under US irradiation without inducing any toxic side effects. The successful development of PMC presents a novel approach for tumor radiosensitization and clearance of tumor stem cells. Moving forward, we aim to further advance the clinical translation research on PMC.

Data Sharing Statement

The detailed experimental steps are provided in the Supporting Information.

Acknowledgments

Disclosure

The authors declare no competing interest in this work.

References

1. Aminabee S, Rao AL, Alimunnisa S. Recent advances in cancer therapy. *Int J Life Sci Pharma Res*. 2020;2:144–146.
2. Korde LA, Somerfield MR, Hershman DL. Use of immune checkpoint inhibitor pembrolizumab in the treatment of high-risk, early-stage triple-negative breast cancer: ASCO guideline rapid recommendation update. *J Clin Oncol*. 2022;40(15):1696–1698. doi:10.1200/JCO.22.00503
3. De Ruysscher D, Niedermann G, Burnet NG, Siva S, Lee AWM, Hegi-Johnson F. Radiotherapy toxicity. *Nat Rev Dis Prime*. 2019;5(1):13. doi:10.1038/s41572-019-0064-5
4. Chen B, Xiao L, Wang W, et al. Bi2–xMnxO3 nanospheres engaged radiotherapy with amplifying DNA damage. *ACS Appl Mater Interfaces*. 2023;15(28):33903–33915. doi:10.1021/acsami.3c06838
5. Huang R-X, Zhou P-K. DNA damage response signaling pathways and targets for radiotherapy sensitization in cancer. *Sig Trans Target Ther*. 2020;5(1):60. doi:10.1038/s41392-020-0150-x
6. Secchi V, Cova F, Villa I, et al. Energy partitioning in multicomponent nanoscintillators for enhanced localized radiotherapy. *ACS Appl Mater Interfaces*. 2023;15(20):24693–24700. doi:10.1021/acsami.3c00853
7. Jabir MS, Sulaiman GM, Taqi ZJ, Li D. Iraqi propolis increases degradation of IL-1beta and NLRC4 by autophagy following Pseudomonas aeruginosa infection. *Microbes Infect*. 2018;20(2):89–100. doi:10.1016/j.micinf.2017.10.007
8. Brand DH, Parker JI, Dearnaley DP, et al. Patterns of recurrence after prostate bed radiotherapy. *Radiother Oncol*. 2019;141:174–180. doi:10.1016/j.radonc.2019.09.007
9. Aponte PM, Caicedo A. Stemness in cancer: stem cells, cancer stem cells, and their microenvironment. *Stem Cells Int*. 2017;3:5619472.
10. Intlekofer AM, Finley LWS. Metabolic signatures of cancer cells and stem cells. *Nat Metab*. 2019;1(2):177–188. doi:10.1038/s42255-019-0032-0

11. Zhang T, Pan Y, Suo M, et al. Photothermal-triggered sulfur oxide gas therapy augments type I photodynamic therapy for potentiating cancer stem cell ablation and inhibiting radioresistant tumor recurrence, Advanced science; 2023.

12. Ning S, Zhang T, Lyu M, Lam JWY, Zhu D, Huang Q. Tang, A type I AIE photosensitiser-loaded biomimetic nanosystem allowing precise depletion of cancer stem cells and prevention of cancer recurrence after radiotherapy. *Biomaterials*. 2023;295:122034. doi:10.1016/j.biomaterials.2023.122034

13. Chen X, Liu B, Tong R, et al. Orchestration of biomimetic membrane coating and nanotherapeutics in personalized anticancer therapy. *Biomater Sci*. 2021;9(3):590–625.

14. Jadhav M, Prasad R, Gandhi M, Srivastava R. Erythrocyte nanovesicles as chemotherapeutic drug delivery platform for cancer therapy. *J Drug Delivery Sci Technol*. 2022;76:103738. doi:10.1016/j.jddst.2022.103738

15. Li JQ, Zhao RX, Yang FM, Qi XT, Ye PK, Xie M. An erythrocyte membrane-camouflaged biomimetic nanoplatform for enhanced chemo-photothermal therapy of breast cancer. *J Mat Chem B*. 2022;10(12):2047–2056. doi:10.1039/D1TB02522H

16. Shen J, Xiong K, Chen Y, Ji L, Chao H. Cancer cell membrane camouflaged iridium complexes functionalized black-titanium nanoparticles for hierarchical-targeted synergistic NIR-II photothermal and sonodynamic therapy. *Biomaterials*. 2021;275:120979.

17. Qian G, Wang J, Yang L, et al. A pH-responsive CaO2@ZIF-67 system endows a scaffold with chemodynamic therapy properties. *J Mater Sci*. 2023;58(3):1214–1228. doi:10.1007/s10853-022-08103-w

18. Huang C, Ding S, Jiang W, Wang F-B. Glutathione-depleting nanoplatelets for enhanced sonodynamic cancer therapy. *Nanoscale*. 2021;13(8):4512–4518. doi:10.1039/D0NR08440A

19. Chen H, Luo X, Huang Q, et al. Platelet membrane fusion liposome loaded with type I AIE photosensitizer to induce chemoresistance cancer pyroptosis and immunogenic cell death for enhancing cancer immunotherapy. *Chem Eng J*. 2023;476:146276. doi:10.1016/j.cej.2023.146276

20. Chen H, Luo X, Cai W, et al. Biomimetic copper-doped polypyrrole nanoparticles for enhanced cancer low-temperature photothermal therapy. *Int J Nanomed*. 2023;18:7533–7541. doi:10.2147/IJN.S428344

21. Huang J, Liu M, Qiu Y, et al. Emerging sonodynamic therapy-based nanomedicines for cancer immunotherapy. *Adv Sci*. 2023;10(2):e2204365. doi:10.1002/advs.202204365

22. Malekmohammadi S, Hadadzadeh H, Rezakhani S, Amirghofran Z. Design and synthesis of gatekeeper coated dendritic silica/titania mesoporous nanoparticles with sustained and controlled drug release properties for targeted synergetic chemo-sonodynamic therapy. *ACS Biomater Sci Eng*. 2019;5(9):4405–4415. doi:10.1021/acsbiomaterials.9b00237

23. Zhang Z, Li B, Xie L, et al. Metal-phenolic network-enabled lactic acid consumption reverses immunosuppressive tumor microenvironment for sonodynamic therapy. *ACS Nano*. 2021;15(10):16934–16945. doi:10.1021/acsnano.1c08026

24. Xu T, Zhao S, Lin C, Zheng X, Lan M. Recent advances in nanomaterials for sonodynamic therapy. *Nano Res*. 2020;13(11):2898–2908.

25. Wang T, Huang C, Ning S, et al. Platelet membrane-coated C-TiO2 hollow nanospheres for combined sonodynamic and alkyl-radical cancer therapy. *Nano Res*. 2022;16:782–791.

26. Ning S, Dai X, Tang W, et al. Cancer cell membrane-coated C-TiO2 hollow nanoshells for combined sonodynamic and hypoxia-activated chemotherapy. *Acta Biomater*. 2022;152:562–574. doi:10.1016/j.actbio.2022.08.067

27. Zhang H, Pan X, Wu Q, Guo J, Wang C, Liu H. Manganese carbonate nanoparticles-mediated mitochondrial dysfunction for enhanced sonodynamic therapy. *Exploration*. 2021;1(2). doi:10.1002/EXP.20210010

28. Kadhem HA, Ibraheem SA, Jabir MS, Kadhim AA, Taqi ZJ, Florin MD. Zinc oxide nanoparticles induces apoptosis in human breast cancer cells via Caspase-8 and P53 pathway. *Nano Biomed Eng*. 2019;11(1). doi:10.5101/nbe.v11i1.p35-43

29. Su J, Sun H, Meng Q, Zhang P, Yin Q, Li Y. Enhanced blood suspensibility and laser-activated tumor-specific drug release of theranostic mesoporous silica nanoparticles by functionalizing with erythrocyte membranes. *Theranostics*. 2017;7(3):523–537. doi:10.7150/thno.17259

30. Liu WL, Zou MZ, Qin SY, et al. Recent advances of cell membrane-coated nanomaterials for biomedical applications. *Adv Funct Mater*. 2020;30(39):2003559.

31. Liu Y, Yang M, Luo J, Zhou H. Radiotherapy targeting cancer stem cells "awakens" them to induce tumour relapse and metastasis in oral cancer. *Int J Oral Sci*. 2020;12(1):19. doi:10.1038/s41368-020-00087-0

32. Huang C, Chen B, Jiang W, et al. Injectable Hydrogel for Cu(2+) controlled release and potent tumor therapy. *Life*. 2021;11:5.

33. Jabir MS, Nayef UM, Abdulkadhim WK, et al. Fe3O4 nanoparticles capped with PEG induce apoptosis in breast cancer AMJ13 cells via mitochondrial damage and reduction of NF-κB Translocation. *J Inorg Organomet Polym Mater*. 2020;31(3):1241–1259. doi:10.1007/s10904-020-01791-4

34. Liang S, Deng X, Chang Y, et al. Intelligent hollow Pt-CuS janus architecture for synergistic catalysis-enhanced sonodynamic and photothermal cancer therapy. *Nano Lett*. 2019;19(6):4134–4145. doi:10.1021/acs.nanolett.9b01595

35. Huang P, Qian X, Chen Y, et al. Metalloporphyrin-encapsulated biodegradable nanosystems for highly efficient magnetic resonance imaging-guided sonodynamic cancer therapy. *J Am Chem Soc*. 2017;139(3):1275–1284. doi:10.1021/jacs.6b11846